Available online at www.sciencedirect.com

ScienceDirect

Catalysis Today 129 (2007) 269–274

CATALYSIS TODAY

www.elsevier.com/locate/cattod

Ultrahigh temperature water gas shift catalysts to increase hydrogen yield from biomass gasification

Agus Haryanto [a,b], Sandun Fernando [a,*], Sushil Adhikari [a]

[a] *Department of Agricultural and Biological Engineering, Mississippi State University, MS 39762, USA*
[b] *Department of Agricultural Engineering, University of Lampung, Indonesia*

Abstract

Noble metal (Rh, Pt, Pd, Ir, Ru, and Ag) and Ni catalysts supported on CeO_2–Al_2O_3 were investigated for water gas shift reaction at ultrahigh temperatures. Pt/CeO_2–Al_2O_3 and Ru/CeO_2–Al_2O_3 demonstrated as the best catalysts in terms of activity, hydrogen yield and hydrogen selectivity. At 700 °C and steam to CO ratio of 5.2:1, Pt/CeO_2–Al_2O_3 converted 76.3% of CO with 94.7% of hydrogen selectivity. At the same conditions, the activity and hydrogen selectivity for Ru/CeO_2–Al_2O_3 were 63.9% and 85.6%, respectively. Both catalysts showed a good stability over 9 h of continuous operation. However, both catalysts showed slight deactivation during the test period. The study revealed that Pt/CeO_2–Al_2O_3 and Ru/CeO_2–Al_2O_3 were excellent ultrahigh temperature water gas shift catalysts, which can be coupled with biomass gasification in a downstream reactor.

Keywords: Hydrogen; Biomass gasification; Ultrahigh temperature; Water gas shift (WGS)

1. Introduction

About 80% of the present world energy demand comes from fossil fuels. The use of fossil fuels, however, has contributed to more than half of all greenhouse gas emissions and a large fraction of air pollutant emissions [1]. Minimizing environmental impacts due to energy production is one of the greatest challenges we face in the 21st century [2]. Also, relying on fossil fuels results in significant challenges with respect to energy security because crude petroleum oil is non-renewable. Hydrogen is considered as an attractive alternative to address these concerns.

Currently, over 96% of hydrogen is produced from steam reforming of fossil fuels at high temperatures with natural gas as the dominant feedstock (48%) followed by heavy oils and naphtha (30%) and coal (18%) [3]. Biomass is an attractive alternative to produce hydrogen [4]. Among all the renewable energy sources, biomass could be the most promising for sustainable hydrogen production [5]. As an energy source, biomass has several important advantages such as biorenewability and environmental friendliness [6,7]. Hydrogen production from biomass is environmentally benign because carbon dioxide (CO_2) released from the process will be reconsumed during photosynthesis, resulting in net zero CO_2 emissions [8].

Thermochemical and biochemical conversion processes are currently used to produce hydrogen from biomass. Gasification is the most mature thermochemical conversion process available [9]. Compared to steam reforming of natural gas, biomass gasification has shown to be lesser dependant on the feedstock cost [10]. At present, the overall cost of producing hydrogen from biomass gasification is higher than that of methane steam reforming [11]. However, future technological developments such as membrane separation and supercritical water gasification are expected to reduce production costs considerably.

Although gasification is a viable technology to produce hydrogen, there are still certain technological challenges to be overcome before this technology becomes feasible for widespread commercialization. Synthesis gas produced from biomass gasification process is generally comprised of mainly carbon monoxide (CO), carbon dioxide (CO_2), hydrogen (H_2), methane (CH_4), water (H_2O), and nitrogen (N_2), and trace amounts of higher hydrocarbons. The amount of hydrogen in

---

[*] Corresponding author. Tel.: +1 662 325 3282; fax: +1 662 325 3853.
E-mail address: sf99@abe.msstate.edu (S. Fernando).

0920-5861/$ – see front matter © 2007 Elsevier B.V. All rights reserved.
doi:10.1016/j.cattod.2006.09.039

Table 1
The absolute amount of ceria and metal loadings

Metal catalyst	Dimensions (mm)		Monolith mass (g)	2.5% Ce (g)	2.5% Metal (g)
	Diameter	Thickness			
Ag-CeO_2/Al_2O_3	20.117	10.693	3.8396	0.0960	0.0960
Rh-CeO_2/Al_2O_3	20.015	10.744	2.8786	0.0720	0.0720
Pt-CeO_2/Al_2O_3	19.812	10.363	2.7149	0.0679	0.0679
Ni-CeO_2/Al_2O_3	19.939	10.261	3.3220	0.0831	0.0831
Pd-CeO_2/Al_2O_3	19.939	10.744	2.6121	0.0653	0.0653
Ru-CeO_2/Al_2O_3	20.066	10.795	3.1751	0.0794	0.0794
Ir-CeO_2/Al_2O_3	19.812	10.846	3.0743	0.0769	0.0769
Pt-Al_2O_3	19.914	10.325	3.7168	0	0.0929

the synthesis gas is relatively low. An alternative way to increase hydrogen yield is employing water gas shift (WGS) reaction (Eq. (1)) in a downstream reactor. The dilemma is that synthesis gas from a gasifier exits at extremely high temperatures (around 800 °C) in comparison to the operating temperatures of the conventional WGS catalysts.

$$CO + H_2O \rightleftharpoons H_2 + CO_2 \quad \Delta H_{298} = -41.2\,\mathrm{kJ/mol} \tag{1}$$

Conventionally, WGS reaction is employed in a two-stage reactor that consists of a high temperature shift (HTS) unit and a low temperature shift (LTS) unit coupled with a cooling system to get the hot gases to cool down to optimum reaction temperatures. The HTS reaction is performed using a Fe–Cr catalyst at a working temperature of approximately 450 °C while the LTS reaction is performed using a Cu–Zn catalyst at approximately 250 °C [12]. Accordingly, the synthesis gas should be cooled to around 450 °C for the HTS to occur and further reduced to 250 °C for the LTS to occur. At commercial scale gasification processes, this step is energy intensive. Our goal in this study was to evaluate non-pyrophoric ultrahigh temperature WGS catalysts that could be directly coupled with biomass gasification unit.

2. Materials and methods

2.1. Catalysts preparation

Catalysts tested in this experiment involved Pt, Rh, Pd, Ir, Ru, Ag, and Ni. Alumina (92%) ceramic foam monoliths containing 8% silica (from Vesuvius Hi Tech Ceramics) having a nominal surface area of ~1 m^2/g and a void fraction of approximately 0.8 was used as the supports for the catalysts. First, the monoliths were saturated with a ceria solution ($Ce(NO_3)_3\cdot 6H_2O$) by wetness incipient technique and dried at 125 °C for an hour. Ceria and metal loadings were 2.5 wt.% of each of the monoliths. Monoliths were then saturated with the metal solution with the same technique as mentioned previously until the required loading was attained. The absolute amount of ceria and metal loadings are presented in Table 1. The monoliths were dried again at 125 °C for 1 h after impregnation to evaporate water. Finally, the catalysts were calcined at 700 °C for 4 h in air. The purpose of the calcination process was to oxidize metal solutions to form metal oxides as well as to facilitate adsorption of the metals to the monolith support. All the required metal solutions for catalysts preparation (H_2PtCl_6, $Rh(NO_3)_3$, $Ni(NO_3)_2\cdot 6H_2O$, $Pd(NO_3)_2$,

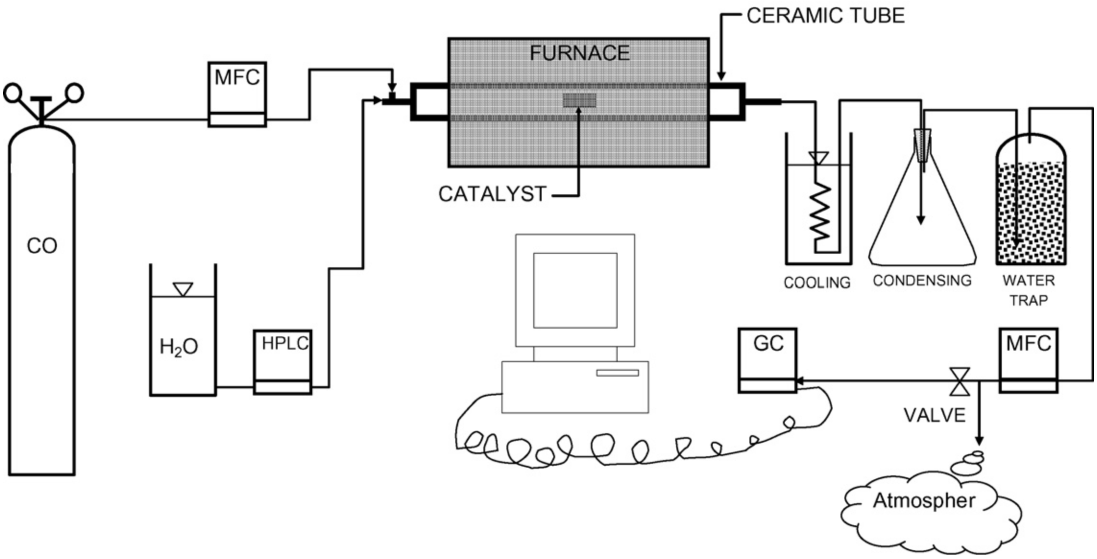

Fig. 1. Experimental set-up for ultrahigh temperature shift WGS reaction.

$AgNO_3$, $HN_4O_{10}Ru$, and H_2Cl_6Ir) were purchased from Sigma–Aldrich. All catalysts were used without being reduced and therefore, all metals were in the oxide form.

2.2. *Catalysts testing*

Catalyst testing was carried out in a tube furnace at temperatures of 700, 500 and 300 °C. Air was purged at 800 °C for an hour in between experiments to oxidize any coke that formed during the previous experiment. The reactor was made of an alumina (99.8%) tube with an outer diameter 1.25 in. A stainless steel tube was placed inside the ceramic tube to hold the catalyst in the center of the reactor. The experimental set-up is depicted in Fig. 1.

The tube furnace was kept for 1 h at the required temperature to stabilize before purging the reactants. Then, the reactants (CO and liquid water) were sent to the reactor. Carbon monoxide flow was controlled using mass flow controller (MFC) at a rate of 120 ml/min. Liquid water was delivered using HPLC pump (LC-20AT, Shimadzu) at a rate of 0.5 ml/min. This was equivalent to GHSV of ~64,000 h^{-1}. The resultant gases, after passing through a condenser and a moisture trap, were analyzed using a gas chromatograph (6890N, Agilent Technologies Incorporated) with a thermal conductivity detector. Three columns from the same company were used in the GC including HP-Molsiv (30 × 0.53), HP-Plot Q (30 × 0.53), and HP-Plot Q (15 × 0.53).

CO conversion and H_2 selectivity were defined as follows:

$$\text{CO conversion} = \frac{F_{\text{CO,in}} - F_{\text{CO,out}}}{F_{\text{CO,in}}} \tag{2}$$

$$\text{H}_2 \text{ selectivity} = \frac{\text{mol H}_2 \text{ yield}}{\text{mol H}_2 \text{ maximum}} \tag{3}$$

where $F_{\text{CO,in}}$ and $F_{\text{CO,out}}$, respectively, denote CO flow rate at the inlet and outlet of the reactor, while mol H_2 maximum in Eq. (3) is based on stoichiometric reaction.

3. Results and discussion

3.1. *Catalyst activity and selectivity*

All catalysts were tested at three different temperatures, i.e., 300, 500, and 700 °C. First, it is important to note that no hydrogen was observed at 300 °C over any of the catalysts attempted. This observation was interesting due to the fact that several of the previous studies suggested otherwise. Wheeler et al. observed a slight CO conversion over several noble metal and Ni catalysts at around 300 °C [13]. On the other hand, noble metal catalysts, and especially Pt/CeO_2, were reported as being good for low temperature shift WGS reaction [14,15]. Recently, Germani and Schuurman reported that $Pt/CeO_2/Al_2O_3$ was very active for the water–gas shift reaction between 250 and 400 °C [16]. Liu et al. also reported that Pt-Ce demonstrated a significant CO conversion after 4000 min at 350 °C [17]. The reason for not observing any CO conversion at 300 °C may be due to the extremely high gas hourly specific velocity (GHSV) applied in our work (~64,000 h^{-1}) compared to, for example, 7000–10,000 h^{-1} in Liu's work [17].

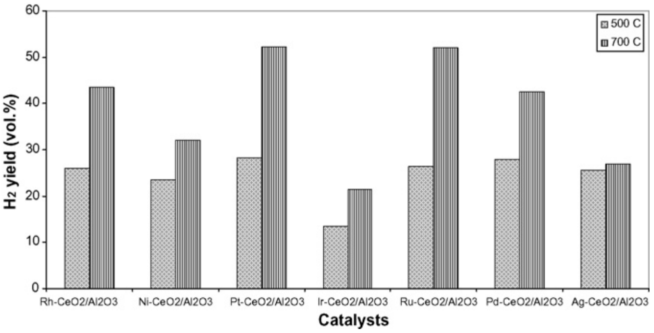

Fig. 2. H_2 yield at 700 and 500 °C for different catalysts.

Fig. 2 depicts the hydrogen yield (presented in vol.% of outlet gas) as a function of operating temperature for different catalysts. It is evident that the reaction produces more hydrogen at 700 °C than that at 500 °C for all catalysts. At 500 °C, hydrogen composition in the product gas was comparable for all catalysts, except for $Ir\text{-}CeO_2/Al_2O_3$. Four catalysts including Rh-, Pt-, Ru- and $Pd\text{-}CeO_2/Al_2O_3$ resulted in hydrogen compositions of more than 40 vol.% at 700 °C. Based on Fig. 1, it can be inferred that $Pt\text{-}CeO_2/Al_2O_3$ and $Ru\text{-}CeO_2/Al_2O_3$ are the best catalysts amongst all catalysts tested. Both catalysts produced hydrogen more than 50 vol.%, specifically 52.2 and 52.0 vol.%, for $Pt\text{-}CeO_2/Al_2O_3$ and $Ru\text{-}CeO_2/Al_2O_3$ catalysts, respectively. Panagiotopoulou and Kondarides recently reported that catalytic activity of Pt and Ru catalysts supported on ''reducible'' metal oxides such as CeO_2 were better than those supported on ''irreducible'' supports such as SiO_2 [18]. Our results suggest that these metal oxide catalysts perform satisfactorily even without reduction at ultrahigh temperatures.

Fig. 3 demonstrates catalysts' selectivity towards hydrogen. All catalysts showed low (<40%) hydrogen selectivity at 500 °C. At 700 °C, however, three catalysts, i.e., Rh-, Pt-, and $Ru\text{-}CeO_2/Al_2O_3$ demonstrated very good selectivity towards hydrogen. Hydrogen selectivity was 94.7% for $Pt\text{-}CeO_2/Al_2O_3$, 85.6% for $Ru\text{-}CeO_2/Al_2O_3$, and 72.7% for $Rh\text{-}CeO_2/Al_2O_3$.

Fig. 4 presents catalysts activity for WGS reaction in terms of CO conversion. Assuming no methane formation, the theoretical equilibrium CO conversion for WGS reaction was estimated to be around 96 and 88% at 500 and 700 °C,

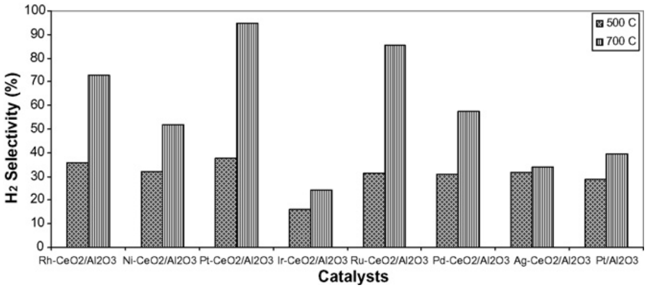

Fig. 3. H_2 selectivity (% of possible maximum) at 700 and 500 °C for different catalysts.

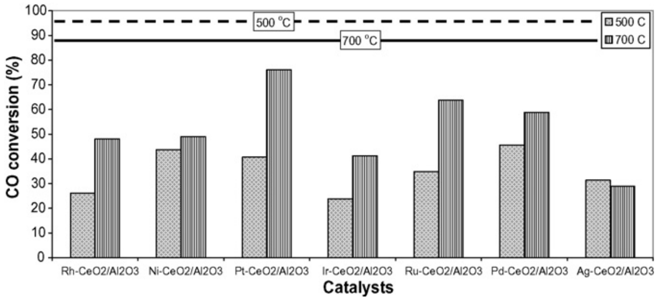

Fig. 4. CO conversion at 700 and 500 °C for different catalysts (horizontal dotted- and solid-line was equilibrium CO conversion at 500 and 700 °C, respectively).

respectively. Based on the reaction conditions in this experiment, the equilibrium CO conversion (X) was calculated using the following expressions:

$$K_{\mathrm{eq}} = \exp\left(-\frac{\Delta G_{\mathrm{R}}}{RT}\right) \tag{4}$$

and

$$K_{\mathrm{eq}} = \frac{X^2}{(1-X)(5.2-X)} \tag{5}$$

where K_{eq} is equilibrium constant, ΔG_{R} the free Gibb's energy of the reaction (J), R the universal gas constant (J mol^{-1} K^{-1}), and T is absolute temperature (K). In this case, ΔG_{R} was calculated from the sum of individual Gibb's energy of the product gases subtracted by the sum of individual Gibb's energy of the reactants. Individual Gibb's energy data were taken from Rosini [19].

The figure demonstrates that at an operating temperature of 500 °C, all catalysts showed relatively low activities compared to theoretical maximum equilibrium conversion possible. Pd-CeO_2/Al_2O_3 showed the highest CO conversion at this temperature which was 45.7%.

At an operating temperature of 700 °C, however, Pt-CeO_2/Al_2O_3, showed the highest conversion of 76.3%. The second highest conversion was exhibited by Ru-CeO_2/Al_2O_3 with CO conversion 63.9%. Wheeler et al. reported that Ni-, Ru-, Pt-, and Rh-Ce catalysts were able to reach equilibrium CO conversion at 600 °C or lower [13]. This disagreement, especially for Ni catalysts, may have resulted from different reaction conditions and catalyst preparation method.

It is important to note that only Ni-CeO_2/Al_2O_3 produced methane. The values were 1.3 and 4.1 vol.% at 500 and 700 °C, respectively. No methane was observed for other catalysts. It is also important that at 300 °C, all catalyst presented extremely low amounts of CO conversion. The average CO conversion at the temperature was 18.7% with the highest being 24.8 for Ru-CeO_2/Al_2O_3 and the lowest being 11.6% for Ni-CeO_2/Al_2O_3. Utaka et al. reported that even though gas product was dominated by CH_4 as a main yield, at 300 °C Ru-Ce catalyst was able to convert more than 80% CO [20]. Li et al. also observed a significant CO conversion at low temperatures over 5% Ni–Ce catalyst, which at 350 °C the catalyst was even able to convert around 95% CO [21]. Differences in gas hourly space velocity, metal loading, and steam to CO ratios are most likely responsible for this disagreement.

3.2. The effect of ceria

The catalytic activity on the WGS reaction was strongly influenced by the kind of support used [14]. This is because the support plays an active role in the reaction [22]. Ceria (CeO_2) has attracted many researchers' attention in recent years, especially as supporting materials for metal catalysts. The promoting roles of cerium oxide involve multiple processes such as the enhancement of the noble metal dispersion, stabilization of the support towards thermal sintering and promoting precious metal catalysts for WGS reaction [14]. Some advantages of ceria-based metal catalysts are reported in the several studies [23–25] including: (i) the ability to operate at a broader range of temperatures; (ii) elimination of the need of reduction process prior to use; (iii) no degradation upon exposure to air (non-pyrophoric); (iv) capability to regenerate deactivated catalysts by simple air atmosphere annealing; (v) the reaction being almost zeroth order in CO on ceria-supported precious metals, due to the redox mechanism in which the metal remains saturated in CO to low CO pressures.

Fig. 5 demonstrates the performances of Pt-Al_2O_3 catalysts with and without ceria in terms of CO conversion, H_2 yield, and H_2 selectivity. It can be seen that the presence of ceria has greatly improved the catalyst performances especially at ultrahigh temperatures. At reaction temperature of 500 °C the effect of ceria is not significant. However, at 700 °C, the addition of ceria to the Pt-Al_2O_3 catalyst has resulted in a considerable increase of CO conversion from 29.1 to 76.3% at 700 °C. At the same temperature, H_2 yield increased from 29.5 to 52.2% and H_2 selectivity increased dramatically from 39.7% to 94.7%. It can be concluded that the presence of ceria significantly improved the performance the catalyst.

It is interesting to note that the performances of the catalysts were greatly influenced by the order of metal and ceria loadings. Previously, we reported the performance of similar catalysts (in this case Rh, Pt and Ir), but ceria and metal were loaded at the same time [26]. The catalysts, however, rapidly lost their activity and H_2 selectivity decreased to around 20% after 540 min on stream (Fig. 6). This implies that the order of

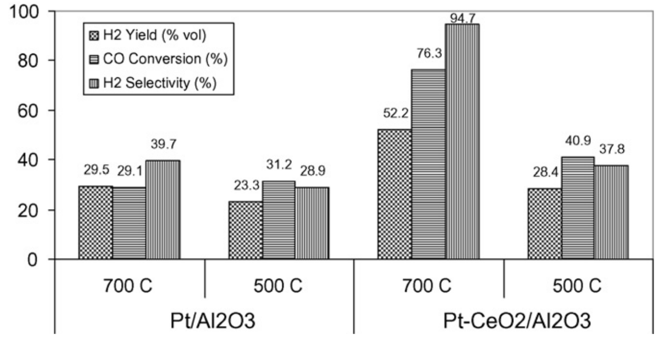

Fig. 5. Performance of Pt-Al_2O_3 and Pt-CeO_2/Al_2O_3 for the WGS reaction at 700 and 500 °C.

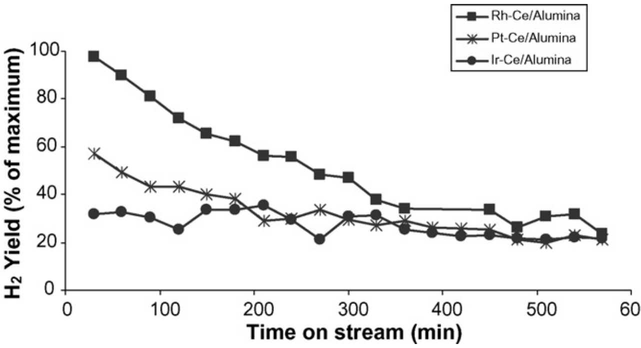

Fig. 6. Hydrogen selectivity vs. time on stream (reaction conditions: 500 °C, steam to CO ratio 6.2:1, and GHSV ~59,300 h^{-1}).

metal loading had a significant effect on the catalyst performance. Impregnating ceria prior to metal loading ensures that ceria retains its function as a support rather than an active catalyst. Also, in this method, it can be safely assumed that the majority of the external surface was coated with the 2.5 wt.% metal fraction where the surface boundaries were mainly comprised of metal–ceria interface. Alternatively, co-impregnation of ceria and metal together let ceria co-express with the metal at a similar intensity possibly reducing the overall amount of metal exposed in the outer most layer resulting in lower conversion instigating coke formation.

3.3. *Catalyst stability*

Based on the previous discussion, it can be surmised that Pt- and Ru-CeO_2/Al_2O_3 performed best amongst the catalysts tested. Therefore, it is important to see the stability of both catalysts. The results are presented in Figs. 7 and 8. Fig. 7 revealed that both catalysts showed a good stability for approximately 560 min time on test apparatus. From Fig. 7, however, it can be seen that both catalysts exhibited a slight decreasing trend in H_2 yield. This may be resulted from coke formation in the catalyst. Other possibility is sintering process because of very high operating temperature. Lassi [27] mentioned that sintering results in the loss of catalyst activity due to the reduction of surface area of the active site. Fig. 8 shows the deactivation problem. It can be examined from Fig. 8 that unreacted CO fraction in the outlet gas increased gradually. For Pt-CeO_2/Al_2O_3 catalyst, the raise in unconverted CO is more pronounced after about 420 min on stream. Liu et al. concluded that deactivation of the Pt/CeO_2 catalyst in WGS reaction was due to the formation of carbonates [17]. Figs. 7 and 8 also depict that Ru-CeO_2/Al_2O_3 presented a better stability than that of Pt-CeO_2/Al_2O_3.

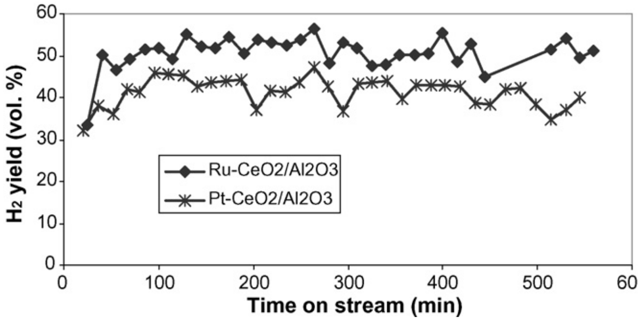

Fig. 7. H_2 yield vs. time on stream for Pt- and Ru-CeO_2/Al_2O_3 (reaction conditions: 700 °C, steam to CO ratio 5.2:1, and GHSV ~64,000 h^{-1}).

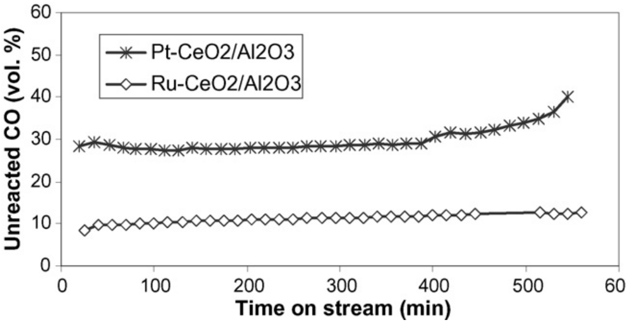

Fig. 8. Unreacted CO vs. time on stream for Pt- and Ru-CeO_2/Al_2O_3 (reaction conditions: 700 °C, steam to CO ratio 5.2:1, and GHSV ~64,000 h^{-1}).

Depending on the above results, it can be inferred that noble metal oxide catalysts in its unreduced form such as Ru- and Pt-CeO_2/Al_2O_3, could be coupled into a synthesis gas stream of a biomass gasifier without the need of the gas stream to be cooled. The catalysts could be conveniently regenerated by a hot stream of air after approximately 9 h of operation. The advantage of the above catalysts is their non-pyrophoricity and the non-requirement to reduce after each run.

4. Conclusion

Noble metal (Rh, Pt, Pd, Ir, Ru, and Ag) and Ni catalysts supported on CeO_2–Al_2O_3 were investigated for water gas shift reaction at ultrahigh temperatures. Based on the observations, it can be concluded that noble metal oxides including Pt, Ru, Rh, and Pd supported on CeO_2/Al_2O_3 demonstrated excellent performance under ultrahigh temperature reaction conditions, i.e., 700 °C, steam to CO ratio 5.2:1, and GHSV ~64,000 h^{-1}. The presence of ceria as a support resulted in a better performance compared to alumina alone. The performances of the catalysts were greatly affected by the order of metal and ceria loading. Ru- and Pt-CeO_2/Al_2O_3 showed superior performance in terms of hydrogen yield, hydrogen selectivity and catalytic activity. Both catalysts are excellent candidates to be coupled to a biomass gasification process with synthesis gas exiting at temperatures above 500 °C.

Acknowledgments

This work was supported by US Department of Energy (Award Number DEFG0204ER63842 04090945). The authors appreciate USDOE and the Mississippi Agricultural and Forestry Experiment Station for supporting this work.

References

[1] J.M. Ogden, Annu. Rev. Energy Environ. 24 (1999) 227.
[2] V. Smil, Annu. Rev. Energy Environ. 25 (2000) 21.

[3] B.E. Logan, Environ. Sci. Technol. (2004) 160A.
[4] D.A. Bowen, F. Lau, R. Zabransky, R. Remick, R. Slimane, S. Doong, Techno-Economic Analysis of Hydrogen Production by Gasification of Biomass, in FY 2003 Annual Progress Report: Hydrogen, Fuel Cells, and Infrastructure Technologies. US DOE, Washington, DC, 2003, p. II-78-81.
[5] S.T. Chaudhari, A.K. Dalai, N.N. Bakhshi, Energy Fuels 17 (2003) 1062.
[6] P.A.M. Claassen, J.B. van Lier, A.M. Lopez Contreras, E.W.J. van Niel, L. Sijtsma, A.J.M. Stams, S.S. de Vries, R.A. Weusthuis, Appl. Microbiol. Biotechnol. 52 (1999) 741.
[7] K. Nath, D. Das, Curr. Sci. 85 (2003) 265.
[8] M.K. Mann, P.L. Spath, Life Cycle Assessment of a Biomass Gasification Combined-Cycle System, National Renewable Energy Laboratory, Golden, Colorado, 1997.
[9] M. Ruggiero, G. Manfrida, Renew. Energy 16 (1999) 1106.
[10] K.A. Adamson, Energy Policy 32 (2004) 1231.
[11] National Research Council and National Academy of Engineering, The Hydrogen Economy: Opportunities, Costs, Barriers, and R&D Needs, The National Academic Press, Washington, DC, 2004.
[12] L. Lyoid, D.E. Ridler, M.V. Twigg, The water gas shift reaction, in: M.V. Twigg (Ed.), Catalyst Handbook, Wolf Publishing Ltd., Frome, England, 1989, p. 283.
[13] C. Wheeler, A. Jhalani, E.J. Klein, S. Tummala, L.D. Schmidt, J. Catal. 223 (2004) 191.
[14] A. Luengnaruemitchai, S. Osuwan, E. Gulari, Catal. Commun. 4 (2003) 215.
[15] G. Jacobs, U.M. Graham, E. Chenu, P.M. Patterson, A. Dozier, B.H. Davis, J. Catal. 229 (2005) 499.
[16] G. Germani, Y. Schuurman, AIChE J. 52 (2006) 1806.
[17] X. Liu, W. Ruettinger, X. Xu, R. Farrauto, Appl. Catal. B: Environ. 56 (2005) 69.
[18] P. Panagiotopoulou, D.I. Kondarides, Catal. Today 112 (2006) 49.
[19] F.D. Rossini, Selected Values of Physical and Thermodynamic Properties of Hydrocarbons and Related Compounds, Carnegie Press, Pittsburg, PA, 1953.
[20] T. Utaka, T. Okanishi, T. Takeguchi, R. Kikuchi, K. Eguchi, Appl. Catal. A: Gen. 245 (2003) 343.
[21] Y. Li, Q. Fu, M. Flytzani-Stephanopoulos, Appl. Catal. B: Environ. 27 (2000) 171.
[22] A. Goguet, F.C. Meunier, J.P. Breen, R. Burch, M.I. Petch, A.F. Ghenciu, J. Catal. 226 (2004) 382.
[23] Q. Fu, H. Saltsburg, M. Flytzani-Stephanopoulos, Science 301 (2003) 935.
[24] S. Swartz, A.-M. Azad, M. Seabaugh, Ceria-based Water–Gas-Shift Catalysts. The 2002 Fuel Cell Seminar, Palm Springs, CA, 2002, p. 587.
[25] S. Hilaire, X. Wang, T. Luo, R.J. Gorte, J. Wagner, Appl. Catal. A: Gen. 258 (2004) 271.
[26] A. Haryanto, S. Fernando, S. Adhikari, Producing sustainable hydrogen from biomass gasification coupled with water gas shift reaction, presentation at ACS National Meeting, Atlanta, April 26–28, 2006.
[27] U. Lassi, Deactivation Correlations of Pd/Rh Three-way Catalysts Designed for Euro IV Emission Limits: Effect of Ageing Atmosphere, Temperature and Time, Dissertation, Department of Process and Environmental Engineering, University Of Oulu, 2003, p. 35.